Enhanced and reduced absorptions via quantum interference: Solid system driven by a rf field

Kazushige Yamamoto, Kouichi Ichimura, and Nobuhiro Gemma
Advanced Research Laboratory, Toshiba Corporation, 1 Komukai Toshiba-cho, Saiwai-ku, Kawasaki 210, Japan
(Received 9 March 1998)

We observed quantum interference effects in steady-state optical absorption in a *V*-type three-level system of $Pr^{3+}:YAlO_3$ where a hyperfine transition between two upper levels was homogeneously broadened by pure dephasing. This *V*-type system was excited by a single driving radio-frequency (rf) field and two probe laser fields (quantum-beat scheme). The probe absorption was constructively or destructively affected by the phase of the driving rf field. In contrast, under two-laser excitation without application of the rf, no absorption change due to electromagnetically induced transparency (EIT) was observed. A comparison of observations and theoretical predictions revealed that the quantum-beat scheme generates quantum interference even when the dephasing rate between the two upper levels is comparable with the Rabi frequency of the probe laser, and completely destroys EIT. [S1050-2947(98)01609-6]

PACS number(s): 42.50.Gy, 32.80.Qk, 76.30.Kg

I. INTRODUCTION

Quantum interference effects, which result in steady-state absorption and emission in atomic gases being destructively or constructively changed, have been widely recognized as fundamental to lasing without inversion (LWI) [1,2], refractive index enhancement [3], and high-efficiency nonlinear susceptibility [4]. The achievement of quantum interference in solid systems is a challenging problem, but it would enable the development of novel devices such as solid-state LWI lasers.

A typical scheme for inducing quantum interference is a three-level system coupled with strong driving laser and weak probe laser [5–7]. In atomic gases, this scheme usually produces the cancellation of probe absorption due to destructive interference (electromagnetically induced transparency; EIT) [5–7]. Absorption cancellation occurs under the conditions of two-photon resonance.

Another scheme for quantum interference is a three-level system with closed excitation by two probe fields and one driving field such as a radio-frequency (rf) field [8–13]. This scheme, which is shown in Fig. 1(a), leads to the quantum-beat laser [8–11]. Kosachiov *et al.* showed that in this ''quantum-beat'' scheme, the two probe absorptions are strongly dependent on the total phase $\Phi = -\phi_1 + \phi_2 + \phi$ of the three electromagnetic fields [12,13], where ϕ_1, ϕ_2, and ϕ are, respectively, the phases of probe 1, probe 2, and the driving field. When the two probes satisfy the two-photon-resonance condition and their phases are fixed, the two probe absorptions can be changed easily both destructively and constructively by the phase ϕ of the driving field.

The aim of this study is to generate quantum interference in steady-state optical absorption in a solid medium using the quantum-beat scheme. Solid media normally show large dephasing, and this generally completely suppresses EIT. Quantum interference due to EIT almost always requires a specific three-level system containing a long-lived level for which the relaxation is very slow. At present, solid systems that have been reported to show EIT are limited to only two examples, ruby [14] and $Pr^{3+}:Y_2SiO_5$ [15,16]. This suggests that in a number of solid systems, dephasing may destroy the atomic coherence required to induce EIT.

The quantum-beat scheme, however, often produces atomic coherence even in collisionally broadened atomic gases with large collisional dephasing as described in Refs. [9,10]. Our approach to quantum interference in solids is to apply this quantum-beat scheme to a special *V*-type three-level system in which the inhomogeneous broadening between the two upper levels is extremely narrow.

In many rare-earth impurity systems in crystals at low temperatures, nuclear-quadrupole resonance between two nearly degenerate hyperfine levels shows an ultranarrow inhomogeneous linewidth of only a few tens of kHz, although the optical transitions have linewidths of the order of a few GHz [17]. This narrow hyperfine transition enables the rf field to directly drive almost all of the impurity ions in a crystal and also allows the two lasers to excite the same ions via two-photon resonance.

These impurity three-level systems may resemble the Doppler-broadened atomic three-level systems with two Zeeman (hyperfine) levels in two nearly degenerate levels being unresolved because of inhomogeneously broadened optical transitions. In Doppler-broadened atomic gases, the modulation of absorption and emission due to interference effects have already been observed as far back as the 1960s [18]. Thus application of the quantum-beat scheme to impurity systems with two nearly degenerate hyperfine levels is a promising approach for achieving solid-state quantum interference.

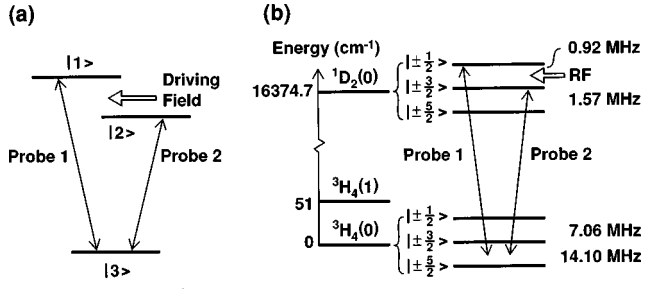

FIG. 1. Schematic energy diagrams for (a) ideal *V*-type three-level atoms and (b) $^3H_4(0)$, $^3H_4(1)$, and $^1D_2(0)$ in $Pr^{3+}:YAlO_3$.

In this article we report an observation of enhanced and reduced absorptions due to quantum interference in a solid medium induced by the quantum-beat scheme. We selected a Pr^{3+}:$YAlO_3$ crystal as the solid medium. This crystal has a *V*-type three-level system in which the hyperfine transition between two upper levels is homogeneously broadened by pure dephasing. The hyperfine transition was driven by a rf field, and excited by two probe lasers.

Many rf-optical double resonance experiments that are relevant to this report have been carried out in rare-earth impurity systems [17]. These works contribute to a detailed understanding of optical pumping (persistent hole burning), photon echo, nuclear-quadrupole interaction, and relaxation phenomena. We, however, focus on quantum interference. A comparison of observations and theoretical predictions revealed that the quantum-beat scheme generates quantum interference even when the dephasing rate between the upper levels is comparable with the Rabi frequency of the probe laser, and completely destroys EIT.

II. EXPERIMENTS

A. Pr^{3+}:$YAlO_3$

Figure 1(b) shows a partial electron-hyperfine energy-level diagram of the impurity ion $Pr^{3+}(I=5/2)$ in the host crystal $YAlO_3$ [17]. The two probe transitions which are to be modified correspond to $^3H_4(0)$-$^1D_2(0)$. This includes nine optical transitions and has a transition frequency of 16 374.7 cm^{-1}. The inhomogeneous linewidth for $^3H_4(0)$-$^1D_2(0)$ is approximately 3 GHz and the optical population lifetime of $^1D_2(0)$ is about 160 μs.

The hyperfine transition, $|\pm 1/2\rangle$-$|\pm 3/2\rangle$ in $^1D_2(0)$, which has a transition frequency of 0.92 MHz was chosen as the transition to be driven by the rf field. The inhomogeneous linewidth is estimated to be approximately 10 kHz [19,20], but the optical transitions of interest are inhomogeneously broadened. The population lifetime between the hyperfine levels in $^1D_2(0)$ is 20–30 μs [20].

The main reason for using the *V*-type Pr^{3+}:$YAlO_3$ system is the ultranarrow inhomogeneous linewidth for the hyperfine transition in $^1D_2(0)$. As mentioned above, this narrow inhomogeneous broadening allows the rf field to directly drive almost all of the Pr^{3+} ions in the crystal and permits the two probes to excite the same ions via two-photon resonance. Selecting a medium of this kind is an essential condition for achieving solid-state quantum interference.

B. Quantum interference experiments

In these experiments using two probe lasers and a single rf field, a 0.05 at. % Pr^{3+}:$YAlO_3$ crystal ($4\times5\times6$ mm^3; Scientific Materials Corp.) with laser-quality polished faces was placed in a liquid-helium cryostat at 8 K. We used a Coherent 699-21 ring-dye laser operating with rhodamine 6G as the source for the two cw probe lasers.

The two probe lasers require different probe frequencies ω_1 and $\omega_2(\omega_1>\omega_2)$ which satisfy the two-photon-resonance condition. The frequency difference $\Delta\omega=\omega_1-\omega_2$ must be equal to the hyperfine transition frequency $\omega_{\rm hf}$. In addition, the two probes must be phase locked together, that is, their phase difference $\Delta\phi=\phi_1-\phi_2$ must always be kept constant. To generate these probes, we applied amplitude modulation to the output of a single laser with acousto-optic modulators (AOM) as described in Ref. [21]. The intensity of the amplitude-modulated output from the AOM is given by

$$I(t)=[A_0\sin\{(\omega_L+\omega_C)t+\phi_0\}]^2\left(\frac{1+\cos 2\omega_{AM}t}{2}\right) \quad (1a)$$

$$=\left(\frac{A_0}{2}\sin\{(\omega_L+\omega_C+\omega_{AM})t+\phi_0\}+\frac{A_0}{2}\sin\{(\omega_L+\omega_C-\omega_{AM})t+\phi_0\}\right)^2, \quad (1b)$$

where ω_L is the laser frequency, ω_C is the carrier frequency driving the AOM, $\omega_{\rm AM}$ is the amplitude-modulation frequency, ϕ_0 is the phase of laser field, and A_0 is a constant.

Equation (1b) shows that the amplitude-modulated output consists of two coherent fields with different frequency components and identical phase components. The two-photon-resonance condition can be satisfied at $\omega_{\rm AM}=\omega_{\rm hf}/2$ by tuning $\omega_{\rm AM}$. Also, the two probes are always phase locked together because $\Delta\phi$ is automatically held at 0°. Using this method, it is also possible to make the two probes overlap perfectly in the sample and to clearly resolve the hyperfine transitions as the $\Delta\omega/2\pi$ accuracy (spectral resolution) is less than 0.1 Hz.

The amplitude-modulated output from the AOM was attenuated to 1–2 mW by neutral density filters. It was focused to a diameter of 100–150 μm within the sample and propagated along the *b* axis [22]. The two probe fields E_1 and $E_2(E_1=E_2)$ were polarized parallel to the *c* axis. The rf field $E_{\rm rf}$ from a rf generator was applied between two copper plates sandwiching the sample. $E_{\rm rf}$ was polarized parallel to the *a* axis. Due to the sample size, the maximum $|E_{\rm rf}|$ was limited to approximately 2×10^2 V/cm. Its frequency $\omega_{\rm rf}$ was tuned to $\omega_{\rm hf}$. For this rf field and the above two probes produced by amplitude modulation, the total phase $\Phi=-\phi_1+\phi_2+\phi=\phi$ was controlled by phase locking between the rf generator and the AOM.

As described later, quantum interference effects were clearly seen in the total steady-state absorption of the two probes as a function of the relative rf phase θ, where $\theta=\phi+\alpha$ and α is a constant. As shown in the inset of Fig. 2, for the closed excitation condition of $\Delta\omega=\omega_{\rm rf}=\omega_{\rm hf}$, the total transmission intensity $I_T(t)$ of the two probes through the sample changed markedly depending on θ. Steady-state probe absorption was estimated from the time-averaged transmission intensity $\langle I_T\rangle$ and from the emission intensity I_E from $^1D_2(0)$ to $^3H_4(1)$.

C. Two-photon-resonance experiments

For the purpose of comparison with quantum interference by three electromagnetic fields, we also investigated EIT using a strong cw driving laser and a weak cw probe laser.

In the experiments, the output of the single ring-dye laser was divided into two beams by a beam splitter, and individual frequency modulations were then applied to these beams using two AOMs. The driving laser frequency ω_D and

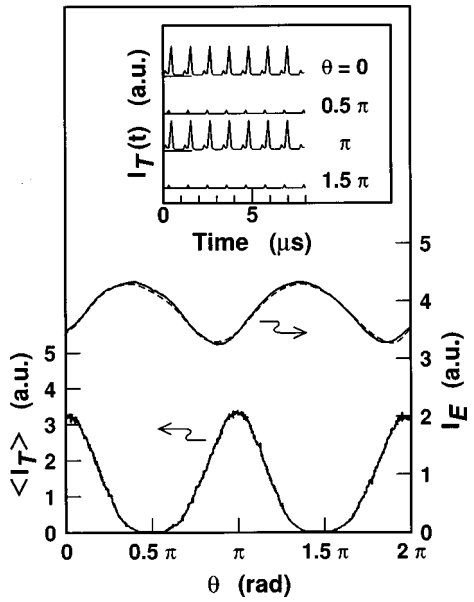

FIG. 2. Individual rf phase dependences of $\langle I_T \rangle$ and I_E (solid lines), measured at $|E_{\rm rf}| = 2\times 10^2$V/cm and $\Delta\omega/2\pi = \omega_{\rm rf}/2\pi = \omega_{\rm hf}/2\pi = 0.92$ MHz. The dashed line is the theoretical I_E-θ curve calculated for $\Omega_{\rm rf} = 40$ kHz, $\Omega_1 = \Omega_2 = 12$ kHz, $\Gamma_{12}^{(L)} = 6$ kHz, $\Gamma_{12}^{(L)} = \Gamma_{13}^{(L)} = 1$ kHz, $\Gamma_{12} = 35$ kHz, $\Gamma_{13} = \Gamma_{23} = 2$ kHz, and $\alpha = -0.12\pi$ using Eq. (5). The inset shows a series of $I_T(t)$ curves at different values of θ.

the probe laser frequency ω_P were independently determined by these AOMs.

The driving and probe beams from the AOMs were adjusted to approximately 20 mW and 0.5 mW, respectively. These two beams were superimposed by another beam splitter. The superimposed beams were focused to a diameter of 100–150 μm in the sample and collinearly propagated along the b axis. The probe field E_P was parallel to the a axis, and perpendicular to the driving field $E_D (E_D \| c)$. E_D was eliminated by a polarizer in front of the detector.

The spectra for the sample, which were strongly coupled by the driving field, were obtained by monitoring the transmitted intensity I_P of the probe from the sample as a function of $\delta\omega = \omega_P - \omega_D$. Typically, ω_P was scanned over a 5-MHz range, while ω_D was held fixed. The spectral resolution was approximately 1 kHz due to the instrument limitations related to the phase lock between these AOMs.

In addition to two-laser excitation, it may be possible to generate EIT by using a rf and a laser. In our rf-optical double resonance measurements, however, EIT was not observed. Due to the large inhomogeneous broadening for the optical transitions, the number of Pr^{3+} ions satisfying the rf-assisted two-photon-resonance conditions would be extremely small in this case, in contrast to the case of two-laser excitation. The small EIT signals are probably eliminated completely by this inhomogeneous broadening.

III. EXPERIMENTAL RESULTS

A. Quantum interference by three electromagnetic fields

Figure 2 shows the individual rf phase dependences of $\langle I_T \rangle$ and I_E, measured at $|E_{\rm rf}| = 2\times 10^2$ V/cm and $\Delta\omega/2\pi = \omega_{\rm rf}/2\pi = \omega_{\rm hf}/2\pi = 0.92$ MHz. As shown, $\langle I_T \rangle$ and I_E were strongly dependent on θ and oscillated with a period of π. The change in steady-state probe absorption was estimated to be approximately 25% from the difference between the maximum and the minimum of the I_E-θ curve. In addition there was a slight phase difference of approximately 0.12π between the two individual curves.

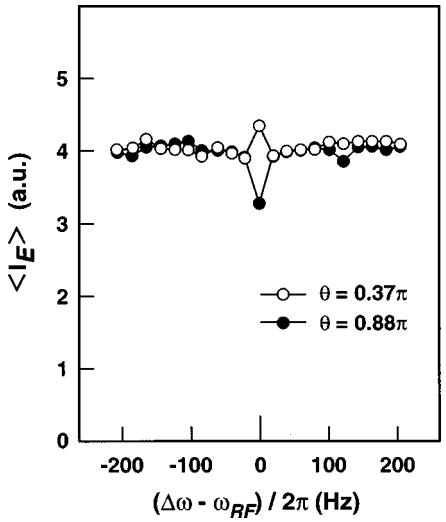

FIG. 3. Excitation spectra at $|E_{\rm rf}| = 2\times 10^2$ V/cm and $\omega_{\rm rf}/2\pi = \omega_{\rm hf}/2\pi = 0.92$ MHz. The open circles correspond to $\theta = 0.37\pi$ and the closed circles to $\theta = 0.88\pi$. Here, $\langle I_E \rangle$ is plotted as a function of the probe detuning $(\Delta\omega - \omega_{\rm rf})/2\pi$.

The above phase-dependent probe absorption is qualitatively explained by assuming two pathways of excitation, one-photon absorption ($|3\rangle \rightarrow |1\rangle$) with the single field $E_1 \sin(\omega_1 t + \phi_0)$ and stepwise dipole absorption ($|3\rangle \rightarrow |2\rangle$ and $|2\rangle \rightarrow |1\rangle$) with the two fields $E_2 \sin(\omega_2 t + \phi_0)$ and $E_{\rm rf} \sin(\omega_{\rm rf} t + \phi)$ [23,24]. If $\omega_1 - \omega_2 = \omega_{\rm rf}$, these two pathways will interfere with each other via the dipole moment, and the steady-state probe absorption will vary depending on the phase difference between the two pathways. The results shown in Fig. 2 indicate quantum interference in optical absorption.

To clarify this point, we investigated I_E as a function of $\Delta\omega$ at the specific phase where the I_E-θ curve showed a maximum or a minimum. The excited-state population produced by the above two pathways oscillates under the unclosed excitation conditions of $\Delta\omega \neq \omega_{\rm rf} = \omega_{\rm hf}$ [23,24]. In this case, the total phase is replaced by $\Phi = -\phi_1 + \phi_2 + \phi - (\omega_1 - \omega_2 - \omega_{\rm rf})t = \phi - (\Delta\omega - \omega_{\rm rf})t$. Thus both I_E and Φ are functions of time. The time-averaged emission intensity $\langle I_E \rangle$ is expected to be relatively independent of $\Delta\omega$ and θ at $\Delta\omega \neq \omega_{\rm rf}$ because the time-averaged total phase is a constant and independent of $\Delta\omega$.

Figure 3 shows the excitation spectra for $\theta = 0.37\pi$ and $\theta = 0.88\pi$. $|E_{\rm rf}|$ and $\omega_{\rm rf}$ are the same as in Fig. 2. For $\theta = 0.37\pi$, the spectrum exhibited a maximum at $\Delta\omega = \omega_{\rm rf}$. In contrast, for $\theta = 0.88\pi$, there was a minimum at $\Delta\omega = \omega_{\rm rf}$. In addition, both spectra showed a similar intensity at $\Delta\omega \neq \omega_{\rm rf}$. This clearly indicates that the enhanced and reduced probe absorptions in Fig. 2 arise from constructive interference and destructive interference, respectively. Thus we have found experimental evidence for quantum interference.

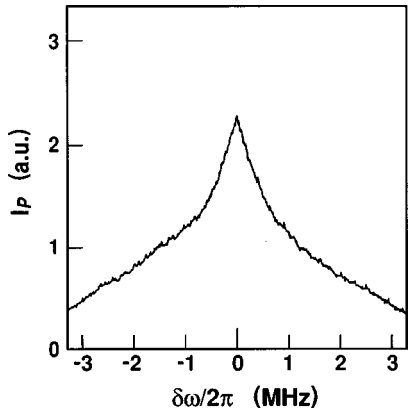

FIG. 4. Transmission intensity I_P of the probe laser as a function of probe detuning $\delta\omega/2\pi$. The driving laser power I_D is approximately 20 mW.

B. Two-photon-resonance by two laser fields

1. Without a rf field

Figure 4 shows the transmission intensity I_P of the probe laser as a function of $\delta\omega/2\pi$, measured for a sample strongly coupled by the driving laser. The incident power I_D of the driving laser is approximately 20 mW.

As shown, there were no EIT signals with sharp peaks at $\delta\omega/2\pi=\pm 0.92$ MHz, ± 1.57 MHz, and ± 2.49 MHz, corresponding to the two-photon resonance in $^1D_2(0)$. In the spectrum, an only broad hole, centered at $\delta\omega/2\pi=0$ MHz, was observed.

This hole at $\delta\omega/2\pi=0$ MHz is explained by saturation effects including spectral hole burning. The hole decayed with two exponential components with lifetimes of approximately 160μs and 6 ms after the driving laser was turned off. These were in good agreement with the optical population lifetime of $^1D_2(0)$ and the population lifetime between the hyperfine levels in $^3H_4(0)$ [25].

EIT in the V-type system requires a fairly narrow linewidth for the transition between the two upper levels, compared with the Rabi frequency for the optical transition determined by the driving laser [7]. The inhomogeneous broadening of approximately 10 kHz for the hyperfine transitions in $^1D_2(0)$ was smaller than the Rabi frequency of approximately 50 kHz estimated from Ref. [21]. Thus the main cause of suppression of EIT could be the homogeneous linewidth for these hyperfine transitions.

The homogeneous linewidth for the hyperfine transitions can be estimated from stimulated Raman spectra [20]. In our stimulated Raman measurements, the spectra were obtained by deducing the contribution of the saturation effects (background probe absorption) from the probe spectrum in Fig. 4 [26]. The power I_D of the driving laser was adjusted to approximately 20 mW.

As shown in Fig. 5(a), weak stimulated Raman signals were observed in the spectrum at $\delta\omega/2\pi=\pm 0.92$ MHz, ± 1.57 MHz, and ± 2.49 MHz, exactly corresponding to the hyperfine transitions in $^1D_2(0)$. The observed transition linewidth of 80–90 kHz [full width at half maximum (FWHM)] indicated that the individual hyperfine transitions were homogeneously broadened by pure dephasing (lifetime broadening is approximately 6 kHz [20]). This linewidth was almost twice as large as the Rabi frequency for the optical transition. These results indicate that pure dephasing in $^1D_2(0)$ suppresses EIT.

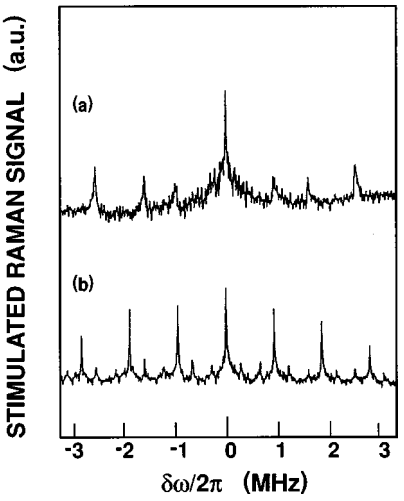

FIG. 5. Stimulated Raman spectra, measured (a) without and (b) with a rf field of $\omega_{rf}/2\pi=0.92$ MHz. Here, $|E_{rf}|=2\times10^2$ V/cm and $I_D\simeq 20$ mW. The spectral resolution for $\delta\omega/2\pi$ is approximately 5 kHz. Note that the signal at $\delta\omega/2\pi=0$ MHz is due to stimulated Rayleigh scattering.

2. With a rf field

Figure 5(b) also shows the measured stimulated Raman spectrum in a rf field of $\omega_{rf}/2\pi=0.92$ MHz. I_D was approximately 20 mW and $|E_{rf}|$ was the same as in the quantum interference experiments.

As shown, the spectrum was markedly different from that obtained without applying a rf field [Fig. 5(a)]. Strong stimulated Raman signals appeared at $\delta\omega/2\pi=\pm 0.92\times N$ MHz($N=1,2,3,\ldots$), whereas the signals at $\delta\omega/2\pi=\pm 1.57$ MHz and ± 2.49 MHz were weakened by the applied rf field. Among these, the two peaks at $\delta\omega/2\pi=\pm 0.92$ MHz were Raman signals from the Pr^{3+} ions subjected to closed excitation by the single rf field and the two lasers. The observed transition linewidth due to pure dephasing was 30–35 kHz. This value was much narrower than that obtained without the rf field.

This unexpected line narrowing indicates that dephasing in $^1D_2(0)$ is partly reduced by adding the rf field to the two lasers, but the details have not been fully understood yet. This reduction of dephasing probably contributes to the quantum interference characteristics shown in Figs. 2 and 3.

In addition, the strong peaks at $\delta\omega/2\pi=\pm 1.84$ MHz and $\delta\omega/2\pi=\pm 2.76$ MHz are Raman signals from Pr^{3+} ions that have interacted with two and three rf photons, respectively. We will report the details of these unusual nonlinear processes separately.

IV. DISCUSSION

To achieve a better quantitative understanding of the quantum interference characteristics in $Pr^{3+}:YAlO_3$ showing large dephasing in $^1D_2(0)$, a comparison was made with theoretical predictions based on the quantum-beat scheme. We investigated both steady-state probe absorption and

atomic coherence in the two upper levels as a function of the rf phase by density matrix analysis. Our analysis was essentially similar to the theoretical analyses of Kosachiov *et al.* [12,13]. The main differences were that we studied the quantum interference characteristics under conditions where the dephasing rate between the two upper levels is comparable to the Rabi frequency of the probe laser (in the analyses by Kosachiov *et al.*, the dephasing rate is assumed to be much smaller than this Rabi frequency), and that we took into account the lifetime effects for the hyperfine transitions and the dephasing effects for the optical transitions.

A. Probe absorption

In the following calculation, we assumed that the perfect triple-resonance condition of $\Delta\omega_{\rm rf}=\Delta\omega_1=\Delta\omega_2=0$, where $\Delta\omega_{\rm rf}=\omega_{\rm rf}-\omega_{12}$, $\Delta\omega_1=\omega_1-\omega_{13}$, $\Delta\omega_2=\omega_2-\omega_{23}$, and $\omega_{mn}(m,n=1,2,3)$ is the transition frequency of $|m\rangle$-$|n\rangle$. In addition, the total phase $\Phi=-\phi_1+\phi_2+\phi$ was taken to be equal to ϕ, because of $\phi_1=\phi_2$ in our experimental conditions. Within a rotating frame, the time-independent interaction Hamiltonian is given by

$$\mathcal{H}_{\rm int}=-\frac{\hbar}{2}\begin{bmatrix}0 & \Omega_{\rm rf}\,e^{-j\phi} & \Omega_1\\ \Omega_{\rm rf}\,e^{j\phi} & 0 & \Omega_2\\ \Omega_1 & \Omega_2 & 0\end{bmatrix}, \tag{2}$$

where $\Omega_{\rm rf}\,e^{-j\phi}$ is the complex Rabi frequency for $|1\rangle$-$|2\rangle$, and Ω_1 and Ω_2 are the Rabi frequencies for $|1\rangle$-$|3\rangle$ and $|2\rangle$-$|3\rangle$, respectively. From $d\rho_{mn}/dt=[\mathcal{H}_{\rm int},\rho]_{mn}/j\hbar$, the evolution equations for the density matrix elements can be written as

$$\frac{d\rho_{11}}{dt}=\frac{j}{2}\Omega_{\rm rf}\,e^{-j\phi}\rho_{21}-\frac{j}{2}\Omega_{\rm rf}\,e^{j\phi}\rho_{12}+\frac{j}{2}\Omega_1(\rho_{31}-\rho_{13})-(\Gamma_{12}^{(L)}+\Gamma_{13}^{(L)})\rho_{11}+\Gamma_{12}^{(L)}\rho_{22}, \tag{3a}$$

$$\frac{d\rho_{22}}{dt}=-\frac{j}{2}\Omega_{\rm rf}\,e^{-j\phi}\rho_{21}+\frac{j}{2}\Omega_{\rm rf}\,e^{j\phi}\rho_{12}+\frac{j}{2}\Omega_2(\rho_{32}-\rho_{23})+\Gamma_{12}^{(L)}\rho_{11}-(\Gamma_{12}^{(L)}+\Gamma_{23}^{(L)})\rho_{22}, \tag{3b}$$

$$\frac{d\rho_{33}}{dt}=-\frac{j}{2}\Omega_1(\rho_{31}-\rho_{13})-\frac{j}{2}\Omega_2(\rho_{32}-\rho_{23})+\Gamma_{13}^{(L)}\rho_{11}+\Gamma_{23}^{(L)}\rho_{22}, \tag{3c}$$

$$\frac{d\rho_{12}}{dt}=\frac{j}{2}\Omega_{\rm rf}\,e^{-j\phi}(\rho_{22}-\rho_{11})+\frac{j}{2}\Omega_1\rho_{32}-\frac{j}{2}\Omega_2\rho_{13}-\Gamma_{12}\rho_{12}, \tag{3d}$$

$$\frac{d\rho_{13}}{dt}=\frac{j}{2}\Omega_{\rm rf}\,e^{-j\phi}\rho_{23}+\frac{j}{2}\Omega_1(\rho_{33}-\rho_{11})-\frac{j}{2}\Omega_2\rho_{12}-\Gamma_{13}\rho_{13}, \tag{3e}$$

$$\frac{d\rho_{23}}{dt}=\frac{j}{2}\Omega_{\rm rf}\,e^{j\phi}\rho_{13}-\frac{j}{2}\Omega_1\rho_{21}+\frac{j}{2}\Omega_2(\rho_{33}-\rho_{22})-\Gamma_{23}\rho_{23}, \tag{3f}$$

where $\Gamma_{12}^{(L)}$ is the decay rate of the population between $|1\rangle$ and $|2\rangle$, $\Gamma_{13}^{(L)}$ and $\Gamma_{23}^{(L)}$ are the respective spontaneous emission rates from $|1\rangle$ and $|2\rangle$ to $|3\rangle$, and Γ_{mn} is the total decay rate for $|m\rangle$-$|n\rangle$ containing the dephasing component.

The probe absorptions I_A and I_E are given by

$$I_A=\Omega_1{\rm Im}\rho_{13}+\Omega_2{\rm Im}\rho_{23}, \tag{4a}$$

$$I_E=\Gamma_{13}^{(L)}\rho_{11}+\Gamma_{23}^{(L)}\rho_{22}. \tag{4b}$$

Here, I_A and $\langle I_T\rangle$ are connected by Lambert's law. To seek steady-state solutions, we set the derivatives in Eq. (3) equal to zero. At $\Omega_1=\Omega_2=\Omega$, $\Gamma_{13}=\Gamma_{23}=\Gamma$, and $\Gamma_{13}^{(L)}=\Gamma_{23}^{(L)}=\Gamma^{(L)}$, we obtain

$$I_A=I_E=\Gamma^{(L)}\left(\frac{AC+2B\sin^2\phi}{AD+3B\sin^2\phi}\right), \tag{5}$$

where $A=(\Omega_{\rm rf}^2+4\Gamma^2)\{\Omega_{\rm rf}^2+\Gamma_{12}(2\Gamma_{12}^{(L)}+\Gamma^{(L)})\}+2\Omega^2\Gamma(2\Gamma_{12}^{(L)}+\Gamma^{(L)}+\Gamma_{12})-\Omega^2(2\Omega_{\rm rf}^2-\Omega^2)$, $B=\Omega_{\rm rf}^2\,\Omega^4(\Gamma_{12}+2\Gamma)^2$, $C=4\Omega^2\Gamma_{12}\Gamma$, and $D=\Gamma^{(L)}\Gamma_{12}(\Omega_{\rm rf}^2+4\Gamma^2)+2\Omega^2\Gamma(\Gamma^{(L)}+3\Gamma_{12})$, respectively.

Equation (5) shows that I_A and I_E are strongly dependent on the $\Omega_{\rm rf}^2\sin^2\phi$ term, which oscillates with period π. This oscillation in absorption versus total phase has been reported by Kosachiov *et al.* [12,13]. As shown in Fig. 2, the theoretical I_E-θ curve, calculated for $\Omega_{\rm rf}=40$ kHz, $\Omega_1=\Omega_2=\Omega=12$ kHz, $\Gamma_{12}^{(L)}=6$ kHz, $\Gamma_{12}^{(L)}=\Gamma_{13}^{(L)}=\Gamma^{(L)}=1$ kHz, $\Gamma_{12}=35$ kHz, $\Gamma_{13}=\Gamma_{23}=\Gamma=2$ kHz, and $\alpha=-0.12\pi$ using Eq. (5), is in good agreement with the experimental curve.

The coincidence of the experimental and theoretical curves indicates that even in conditions where the dephasing rate (approximately Γ_{12}) between the two upper levels is comparable to the Rabi frequency of the probe laser, the probe absorption is constructively or destructively changed by the rf phase. In contrast, absorption cancellation due to EIT is completely destroyed under these conditions ($\Gamma_{12}\simeq\Omega_1,\Omega_2$) [7]. For achieving quantum interference in solids with large dephasing, the quantum-beat scheme using three electromagnetic fields is likely to be much more effective than the EIT scheme using two fields.

The parameters chosen for use in the above calculations are similar to those in the experiments, except for $\Omega_{\rm rf}$ and Γ which are the fitting parameters. The small Γ implies that the optical homogeneous linewidth is as narrow as the lifetime broadening. From optical free induction decay measurements using an intense laser (approximately 50 mW) at 8 K, however, the linewidth was estimated to be approximately 100 kHz. The closed excitation by the rf field and the two lasers may cause the suppression of the optical homogeneous linewidth as well as the unexpected line narrowing for the hyperfine transitions in $^1D_2(0)$ as shown in Fig. 5, but the details have not been fully understood yet.

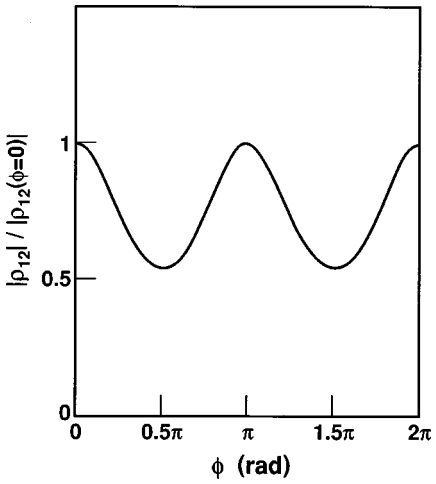

FIG. 6. Theoretical $|\rho_{12}|$-ϕ curve calculated for $\Omega_{rf}=40$ kHz, $\Omega_1=\Omega_2=12$ kHz, $\Gamma_{12}^{(L)}=6$ kHz, $\Gamma_{12}^{(L)}=\Gamma_{13}^{(L)}=1$ kHz, $\Gamma_{12}=35$ kHz, and $\Gamma_{13}=\Gamma_{23}=2$ kHz using Eq. (6). The curve is normalized against the maximum value (value at $\phi=0,\ \pi$).

B. Upper level coherence

Kosachiov *et al.* showed that in the *V*-type system, probe absorption is governed by the atomic coherence between the two upper levels [12,13]. Phase modulation of the rf field causes the destruction and restoration of this upper level coherence. The upper level coherence is given by the ρ_{12} component in Eq. (3), which can be expressed as

$$\rho_{12}=\left(\frac{AE-jFe^{-j\phi}\sin\phi}{AD+3B\sin^2\phi}\right), \tag{6}$$

where $E=2\Omega^2\Gamma^{(L)}\Gamma$ and $F=4\Omega_{rf}^2(\Omega_{rf}^2-\Omega^2+4\Gamma^2)(\Gamma_{12}+2\Gamma)$, respectively. In Eq. (6), the modulus $|\rho_{12}|$ shows the degree of upper level coherence.

Figure 6 shows the theoretical $|\rho_{12}|$-ϕ curve. All the parameters used here are the same as in the above I_E calculations. As shown, $|\rho_{12}|$ was strongly dependent on ϕ. It exhibited maximums at $\phi=0$ and $\phi=\pi$, but minimums at $\phi=0.5\pi$ and $\phi=1.5\pi$.

The upper level coherence generates a coherent superposition of $(|1\rangle-|2\rangle)/\sqrt{2}$ in the two upper levels. This eigenstate causes reduced absorption, because the upper levels are optically decoupled from the lower level $|3\rangle$. Taking into account the experimental results, the upper level coherence at $\phi=0$ and $\phi=\pi$ yields reduced probe absorption in the $\langle I_T\rangle$-θ and I_E-θ curves in Fig. 2 (destructive interference). In contrast, the destruction of the coherence at $\phi=0.5\pi$ and $\phi=1.5\pi$ produces enhanced probe absorption in these curves (constructive interference).

In addition, the result in Fig. 6 directly shows that the upper level coherence can still be controlled by ϕ even in conditions where dephasing between the upper levels is large enough to destroy EIT. In other words, the upper level coherence generated by the quantum-beat scheme overcomes this dephasing. This is a distinguishing characteristic of the quantum-beat scheme.

Finally, it should be noted that our arguments are limited to the contribution of quantum interference effects to probe absorption. Quantum interference also appears in spontaneous emission [27]. In this case, the decay rates, including the spontaneous emission rates, are thought to be dependent on the phase of the rf field and these are not constant as assumed in the above analysis. It seems that the slight phase difference between the two experimental curves in Fig. 2 is closely related to this effect.

V. CONCLUSION

We have succeeded in generating quantum interference in steady-state optical absorption in a *V*-type three-level system of Pr^{3+}:$YAlO_3$ showing large dephasing in the upper levels. This was done using closed excitation by a single rf field and two lasers (quantum-beat scheme). The absorption was constructively or destructively changed depending on the phase of the rf field. Comparison with the EIT characteristics produced by the two lasers suggested that the quantum-beat scheme was effective in achieving quantum interference in solid mediums with large dephasing. In addition, density matrix analysis indicated that even in conditions where the dephasing rate is comparable to the Rabi frequency of the laser, absorption is strongly dependent on the atomic coherence induced in the solids by the phase of the rf field. We expect it to be possible to generate quantum interference in various solid systems using the quantum-beat scheme. We also expect the introduction of atomic coherence into solids to dramatically change not only optical properties but also other characteristics such as magnetic and dielectric properties.

[1] S. E. Harris, Phys. Rev. Lett. **62**, 1033 (1989).
[2] O. A. Kocharovskaya and Ya. I. Khanin, Pis'ma Zh. Éksp. Teor. Fiz. **48**, 581 (1988) [JETP Lett. **48**, 630 (1988)].
[3] M. O. Scully, Phys. Rev. Lett. **67**, 1855 (1991).
[4] K. Hakuta, L. Marmet, and B. P. Stoicheff, Phys. Rev. Lett. **66**, 596 (1991).
[5] A. Imamoğlu and S. E. Harris, Opt. Lett. **14**, 1344 (1989).
[6] A. Imamoğlu, J. E. Field, and S. E. Harris, Phys. Rev. Lett. **66**, 1154 (1991).
[7] S. E. Harris, Phys. Today **50** (7), 36 (1997).
[8] M. O. Scully and M. S. Zubairy, Phys. Rev. A **35**, 752 (1987).
[9] M. O. Scully, S.-Y. Zhu, and A. Gavrielides, Phys. Rev. Lett. **62**, 2813 (1989).
[10] E. E. Fill, M. O. Scully, and S.-Y. Zhu, Opt. Commun. **77**, 36 (1990).
[11] J. A. Bergou and P. Bogár, Phys. Rev. A **43**, 4889 (1991).
[12] D. V. Kosachiov, B. G. Matisov, and Yu. V. Rozhdestvensky, Opt. Commun. **85**, 209 (1991).
[13] D. V. Kosachiov, B. G. Matisov, and Yu. V. Rozhdestvensky, J. Phys. B **25**, 2473 (1992).
[14] Y. Zhao, C. Wu, B. S. Ham, M. K. Kim, and E. Awad, Phys. Rev. Lett. **79**, 641 (1997).

[15] B. S. Ham, M. S. Shahriar, and P. R. Hemmer, Opt. Lett. **22**, 1138 (1997).
[16] B. S. Ham, P. R. Hemmer, and M. S. Shahriar, Opt. Commun. **144**, 227 (1997).
[17] For example, see L. E. Erickson, Phys. Rev. B **19**, 4412 (1979); A. A. Kaplyanskii and R. M. Macfarlane, *Spectroscopy of Solids Containing Rare Earth Ions* (North-Holland, Amsterdam, 1987).
[18] For reviews of early studies on quantum interference effects in atomic gases, see G. W. Series, Physica (Amsterdam) **33**, 138 (1967); E. B. Aleksandrov, Usp. Fiz. Nauk **7**, 595 (1972) [Sov. Phys. Usp. **15**, 436 (1973)].
[19] M. Mitsunaga, E. S. Kintzer, and R. G. Brewer, Phys. Rev. B **31**, 6947 (1985).
[20] Y. S. Bai and R. Kachru, Phys. Rev. Lett. **67**, 1859 (1991).
[21] T. Blasberg and D. Suter, Phys. Rev. B **51**, 6309 (1995).
[22] R. Diehl and G. Brandt, Mater. Res. Bull. **10**, 85 (1975).
[23] N. Ph. Georgiades, E. S. Polzik, and H. J. Kimble, Opt. Lett. **21**, 1688 (1996).
[24] N. Ph. Georgiades, E. S. Polzik, and H. J. Kimble, Phys. Rev. A **55**, R1605 (1997).
[25] T. Blasberg and D. Suter, Chem. Phys. Lett. **215**, 668 (1993).
[26] To separate stimulated Raman signals from background probe absorption, the driving beam is gated by the AOM to produce a pulse train. The transmitted intensity $I_P(t)$ of the probe beam from the sample suddenly decreases at the end of each pulse of the driving beam. This intensity drop ΔI_P of the probe beam corresponds to the stimulated Raman signal. ΔI_P can be obtained by deducing $I_P(t)$ immediately after the end of the pulse from the $I_P(t)$ just before that. In the measurements, these two probe intensities were independently collected by two boxcar integrators. The two gates of the integrators were set at intervals of 5μs before and after the end of the pulse, and their widths were both 5μs. Two outputs from the integrators were sent to a differential amplifier. ΔI_P was estimated from the output of this amplifier. The stimulated Raman spectra were obtained from ΔI_P as a function of $\delta\omega/2\pi$.
[27] For example, see M. A. G. Martinez, P. R. Herczfeld, C. Samuels, L. M. Narducci, and C. H. Keitel, Phys. Rev. A **55**, 4483 (1997); D. A. Cardimona, M. G. Raymer, and C. R. Stroud, Jr., J. Phys. B **15**, 55 (1982); S.-Y. Zhu and M. O. Scully, Phys. Rev. Lett. **76**, 388 (1996).